42 (1), 2018: 32-38

https://journals-crea.4science.it/index.php/asr

Research paper

Use of Sentinel-2 for forest classification in Mediterranean environments

Nicola Puletti[1], Francesco Chianucci[2], Cristiano Castaldi[1*]

Received 19/09/2017 - Accepted 27/10/2017 - Published online 20/06/2018

Abstract - Spatially-explicit information on forest composition provides valuable information to fulfil scientific, ecological and management objectives and to monitor multiple changes in forest ecosystems. The recently developed Sentinel-2 (S2) satellite imagery holds great potential for improving the classification of forest types at medium-large scales due to the concurrent availability of multispectral bands with high spatial resolution and quick revisit time. In this study, we tested the ability of S2 for forest type mapping in a Mediterranean environment. Three operational S2 images covering different phenological periods (winter, spring, summer) were processed and analyzed. Ten 10 m and 20 m bands available from S2 and four vegetation indices (VIs) were used to evaluate the ability of S2 to discriminate forest categories (conifer, broadleaved and mixed forests) and four forest types (beech forests; mixed spruce-fir forests; chestnut forests; mixed oak forests). We found that a single S2 image acquired in summer cannot discriminate neither the considered forest categories nor the forest types and therefore multitemporal images collected at different phenological periods are required. The best configuration yielded an accuracy > 83% in all considered forest types. We conclude that S2 can represent an effective option for repeated forest monitoring and mapping.

Keywords - Forest Classification; European Forest Types; Multispectral satellite imagery; Jeffries-Matusita (J-M) distance test; Random Forest

Introduction

Classification of forest categories and types is strongly required for addressing a wide range of ecological questions related to the determination of forest classes and/or successional stages (Laurin et al., 2013), rate of afforestation/deforestation (Hirose et al., 2016; Omruuzun et al., 2015), functional composition (Laurin et al., 2016) and global environmental changes (Trumbore et al., 2015). All these kinds of application require very fine mapping and monitoring of forest types, which have so far been limited by the spectral, spatial and temporal resolution available from current satellite open access data (e.g., Landsat, MODIS).

Previous studies using satellite multispectral sensors indicate that the visible and near-infrared wavelength regions are important for forest classification (Immitzer et al., 2012; Moore and Bauer, 1990; Waser et al., 2014). However, very few studies using multispectral sensors have evaluated the importance of red-edge bands for forest classification (e.g., Adelabu et al., 2013). As alternative to satellite remote sensing, unmanned aerial vehicles have recently gained increasing attention to obtain detailed information at local scale and at flexible temporal resolution, but their large scale applications in forestry are still at an experimental stage (Chianucci et al., 2016). Accurate discrimination of forest types is also essential for sustainable forest management and planning (Barbati et al., 2014), for estimating carbon stock (Noguiera et al., 2005) and for modelling the distribution of species and communities (Foody et al., 2003). Therefore, there is an increasing demand in both open access high quality data and quick turnaround series from remote sensing sensors for accurate mapping and monitoring of forest environments. This is particularly relevant for Mediterranean forests, which are characterized by high level of complexity (e.g., large number of species and variable canopy densities), which can complicate the discrimination of forest types from optical satellite imagery (Bajocco et al. 2013; Maselli et al., 2009; Pignatti et al., 2009). For example, previous studies indicated that Mediterranean forest types are often characterized by very high canopy density (Leaf Area Index, LAI > 5 m^2 m^{-2}, Chianucci, 2016; Chianucci et al., 2014; Chianucci and Cutini, 2013; Cinnirella et al., 2002; Thimonier et al., 2010), which can limit the retrieval of optical information from satellite data. Indeed, optical measures often saturate at leaf area index values of about 5 (Thenkabail et al., 2000), while vegetation indices using near-infrared (NIR) bands may saturate at

[1] CREA Research Centre for Forestry and Wood, Arezzo, Italy
[2] CREA Research Centre for Agriculture and Environment, Rome, Italy
*cristiano.castaldi@crea.gov.it

http://dx.doi.org/10.12899/ASR-1463

lower values (Davi et al., 2006; Turner et al., 1999). In addition, Mediterranean forests exhibits different phenological patterns according to forest categories and types, and therefore accurate temporal resolution data are strongly required for discriminating different forest types in these environments.

The recent Sentinel-2 (S2) mission, which started June 2015, holds great potential for the fine classification and monitoring of forest types on large scales (Baillarin et al., 2012). Even if S2 does not carry on a hyperspectral sensor, it was specifically conceived for vegetation sensing purposes and offers innovative features for environmental remote sensing (Immitzer et al., 2016). S2 can combine high spatial resolution, wide coverage and quick revisit time (about 5 days), which offers unprecedented opportunities for fine discrimination of land-cover classes. S2 carries a multispectral sensor with 13 bands, from 0.443 to 2.190 µm. The visible R, G, B and the NIR bands are available at a 10 m spatial resolution, highly suitable for application in vegetation canopies. Four red-edge bands at 20 m spatial resolution are also available and are particularly suited for chlorophyll content analysis and to parametrize ecophysiological large-scale models. Despite its potential, few studies have evaluated the ability of S2 in forest mapping and monitoring (Nelson, 2017). Immitzer et al. (2016) used actual S2 data for forest mapping, but they used pre-operational data without radiometric and geometric corrections, which hampers the comparison with other datasets. Indeed, the pre-operational data often showed artifacts which limit the consistency of the remotely-sensed information available from S2 (Immitzer et al., 2016; Vaiopoulos and Karantzalos, 2016). In addition, because of the relatively recent release of S2, most previous studies were based on simulated S2 data (e.g. Hill, 2013; Laurin et al., 2016).

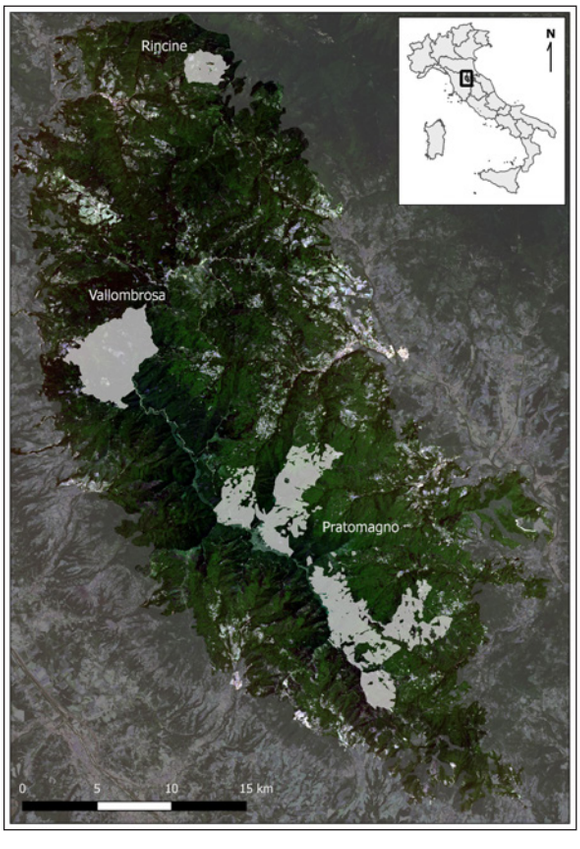

Figure 1 - True colour composition of the entire study area from Sentinel-2 imagery. The Regions of Interest (ROI) have been labelled in white.

The main objective of this study was to evaluate the capability of S2 operational data (i.e. after the correction from ESA) in classifying both forest categories (pure coniferous forests, pure broadleaves forests, and mixed forests) and European Forest Types (EFT; Barbati et al 2014) in a Mediterranean environment, which has not been possible before due to limited pre-operational S2 data availability. Because of the different phenological patterns of Mediterranean forests, we also compared the use of multitemporal data versus single time data for the discrimination of forest categories and types from S2.

2. Material and methods

2.1. Test site

The study was carried out in an extensive forest area (about 470 km^2) located in the Eastern part of the Tuscany Region (Figure 1). A Region Of Interest (ROI) made of 1,061 stands distributed over three forest compartments (3,960 ha)was created. The forest types that covered the study area, according to the European classification (Barbati et al., 2014), are the Apennine-Corsican mountainous beech forests (EFT code 7.3), the Thermophilous deciduous forests dominated by chestnut (EFT code 8.7), the Subalpine and mountainous spruce and mountainous mixed spruce-silver fir forest (EFT code 3.2), and the Turkey oak, Hungarian oak and Sessile oak forest (EFT code 8.2), which cover 13.4%, 35.3%, 8.9%, and 38.1% of the forest surface in the AOI, respectively.

2.2. S2 products collection and pre-processing

Sentinel-2 features 13 spectral bands with 10, 20 and 60 m spatial resolution (Table 1) at 12 bit radiometric resolution. For the remainder of the analysis, we focused only on 10 m and 20 m bands (Table 1). The three 60 m spatial resolution bands were not used in this study because they are primarily relevant for atmospheric corrections. In this work, three S2 products were downloaded as Level-1C Top-of-Atmosphere reflectance products from the Scientific Hub (https://scihub.copernicus.eu): one relative to winter (January, 2017, product code "S2A MSIL1C 20170104T101402 N0204 R022 T32TQP 20170104T101405"), one to spring (March,

Table 1 - Spectral bands available from Sentinel-2. Only bands with finer spatial resolution (i.e. 10 m and 20 m) have been used in this work.

Sentinel-2 Bands	Central Wavelength (μm)	Spatial Resolution m
Band 1 - Coastal aerosol	0.443	60
Band 2 - Blue	0.490	10
Band 3 - Green	0.560	10
Band 4 - Red	0.665	10
Band 5 - Red Edge	0.705	20
Band 6 - Red Edge	0.740	20
Band 7 - Red Edge	0.783	20
Band 8 - NIR	0.842	10
Band 8A - Red Edge	0.865	20
Band 9 - Water vapour	0.945	60
Band 10 - SWIR - Cirrus	1.375	60
Band 11 - SWIR	1.610	20
Band 12 - SWIR	2.190	20

2017, product code "S2A MSIL1C 20170315T101021 N0204 R022 T32TQP 20170315T101214") and one to summer (June, 2017, product code "S2A MSIL1C 20170613T101031 N0205 R022 T32TQP 20170613T101608").

The products were resampled at a resolution of 10 m by the Sentinel Application Platform (SNAP), available at the ESA website (http://step.esa.int/main/toolboxes/snap). Finally, the 10 bands were imported in ENVI software, stacked and cropped over the area of interest.

2.3. Model assessment

The separability between forest categories (pure coniferous forests, pure broadleaves forests, and mixed forests) and forest types (EFTs) was evaluated. Firstly, we define the classification ability of winter, spring and summer products separately using ten S2 bands resampled at 10 m. Vegetation indices were also included in a second step of the analysis; considering the used spectral bands, we computed the Normalized Difference Vegetation (NDVI), the Simple Ratio (SRI), the red-edge Normalized Difference Vegetation (RENDVI) and the Anthocyanin Reflectance Index 1 (ARI1) indices (Table 2).

As suggested from other experiences (Puletti et al., 2016; Laurin et al., 2016), a preliminary analysis on ROIs separability was performed by Jeffries-Matusita (J-M) distance test applied to the validation set (see Table 3). The value of the J-M measurement ranges from 0 to 2.0 and indicates how the selected ROI pairs are statistically separated: values above 1.8 indicate a statistically good separability (Richards and Jia, 1999). As a third step, we repeated the separability analysis by combining (layer-stack) the three S2 images, to explore the capability of S2 to improve the forest type classification using multitemporal information. All J-M analyses were performed in ENVI software.

Table 2 - The vegetation indices calculated from S2 imagery. ρ refers to the reflectance value of the S2 band considered. For the identification of the band number used, see Table

Vegetation Index	Formula
NDVI	$(\rho_{842}-\rho_{665})/(\rho_{842}+\rho_{665})$
SRI	ρ_{842}/ρ_{665}
RENDVI	$(\rho_{740}-\rho_{705})/(\rho_{740}+\rho_{705})$
ARI1	$(1/\rho_{560})-(1/\rho_{705})$

Table 3 - Number of 10x10 m pixels used in this study as ROI for forest category classification, distinguished by training and validation sets.

Forest Compartment	Forest category	Training set (number)	Validation set (number)	Total number of pixels
Pratomagno	coniferous	24,684	10,579	35,263
	broadleaves	75,230	32,242	107,472
	mixed	78,437	33,616	112,053
Rincine	coniferous	8,862	3,798	12,660
	broadleaves	2,770	1,187	3,957
	mixed	7,244	3,105	10,349
Vallombrosa	coniferous	25,901	11,100	37,001
	broadleaves	17,003	7,287	24,290
	mixed	37,028	15,869	52,897
	Total	277,159	118,783	395,942

Table 4 - Number of 10x10 m pixels used in this study as ROI for forest type classification (EFT), distinguished by training and validation sets. EFT 3.2: Subalpine and mountainous spruce and mountainous mixed spruce-silver fir forest; EFT 7.3: Apennine-Corsican mountainous beech forest; EFT 8.2: Turkey oak, Hungarian oak and Sessile oak forest; EFT 8.7: Chestnut forest.

	Training set (number)	Validation set (number)	Total number of pixels
EFT 3.2	29,336	12,572	41,908
EFT 7.3	85,850	36,793	122,643
EFT 8.2	6,944	2,976	9,920
EFT 8.7	49,935	21,401	71,336
Total	172,065	73,742	245,807

The best configuration obtained from J-M distance test was used to classify the S2 products using the Random Forest method (Breiman, 2001). This method requires two input parameters: the number of predictor variables performing the data partitioning at each node and the total number of trees to be grown in the model run. For categorical classification based on the Random Forest model, the number of predictor variables was set as the square root of the number of predictor within the dataset used in the study (Liaw and Wiener, 2002).

2.4. Model evaluation

The ROI pixels were randomly divided into training and validation sets (Table 3 and Table 4), using a proportion of 70% and 30% respectively. The classification analysis was performed using the 'randomForest' package in R (R Core Team, 2017). The Random Forest model was built over the training set; the Overall Accuracy (OA), Producer Accuracy (PA), User Accuracy (UA) and Kappa coefficient of the classification were computed using information from the contingency matrix, obtained applying the model to the entire validation set (Congalton, 1991).

Table 5 - J-M scores for pairs of forest groups (Con-pure conifers; Broad-pure broadleaves; Mix-mixed) using single date and multitemporal S2 imagery.

Input	Pair	Winter	Spring	Summer	Multitemporal
10 bands	Mix vs Con	0.67	0.56	0.47	1.14
	Mix vs Broad	1.30	1.52	0.89	1.87
	Broad vs Con	1.71	1.83	1.59	1.98
10 bands	Mix vs Con	0.94	1.77	0.59	1.95
+ NDVI	Mix vs Broad	1.32	1.94	1.09	1.97
	Broad vs Con	1.80	1.99	1.71	1.99
10 bands	Mix vs Con	0.94	1.77	0.52	1.92
+ SRI	Mix vs Broad	1.31	1.82	0.91	1.94
	Broad vs Con	1.80	1.99	1.61	1.99
10 bands	Mix vs Con	0.93	1.80	0.58	1.95
+ RENDVI	Mix vs Broad	1.32	1.95	1.04	1.98
	Broad vs Con	1.80	1.99	1.69	1.99
10 bands	Mix vs Con	0.73	0.77	0.52	1.30
+ ARI1	Mix vs Broad	1.33	1.54	0.98	1.88
	Broad vs Con	1.77	1.87	1.60	1.98
10 bands	Mix vs Con	1.21	1.96	0.69	2.00
+ 4 VIs	Mix vs Broad	1.54	2.00	1.25	2.00
	Broad vs Con	1.93	2.00	1.78	2.00

2.5 Map production

The validated model was applied to the entire study area (470 Km^2) and 10 m spatial resolution maps for both forest categories and EFTs have been obtained.

3. Results

3.1. J-M test

Results from spring image indicated that the single image 10 bands discriminated well between broadleaved and needleleaved forests, regardless of the phenological acquisition period, but did not differentiate mixed forests (Table 5). Including the vegetation indices only slightly increased the separability between these classes, which was significant only for spring image using RENDVI. When exploiting the multitemporal information of S2, the J-M separability markedly improved compared with the single date analysis (Table 5). The solely combination of bands did not allow the discrimination of the forest categories (J-M value of 1.14 for mixed vs coniferous, see Table 5), and inclusion of VIs was therefore required (Table 5).

Table 6 - J-M scores for pairs of selected EFT. EFT 3.2: Subalpine and mountainous spruce and mountainous mixed spruce-silver fir forest; EFT 7.3: Apennine-Corsican mountainous beech forest; EFT 8.2: Turkey oak, Hungarian oak and Sessile oak forest; EFT 8.7: chestnut forest.

Input	Pair	J-M score
10 bands (spring) + 10 bands (summer)	EFT 3.2 / EFT 7.3	1.93
	EFT 3.2 / EFT 8.2	1.96
	EFT 3.2 / EFT 8.7	1.78
	EFT 7.3 / EFT 8.2	1.98
	EFT 7.3 / EFT 8.7	1.92
	EFT 8.2 / EFT 8.7	1.63
10 bands + RENDVI (spring) + 10 bands + RENDVI (summer)	EFT 3.2 / EFT 7.3	2.00
	EFT 3.2 / EFT 8.2	1.98
	EFT 3.2 / EFT 8.7	1.88
	EFT 7.3 / EFT 8.2	2.00
	EFT 7.3 / EFT 8.7	1.99
	EFT 8.2 / EFT 8.7	1.73

As described in Figure 2, the same procedure has been adopted for EFTs classification (Table 6). In this case, due to results obtained in the first

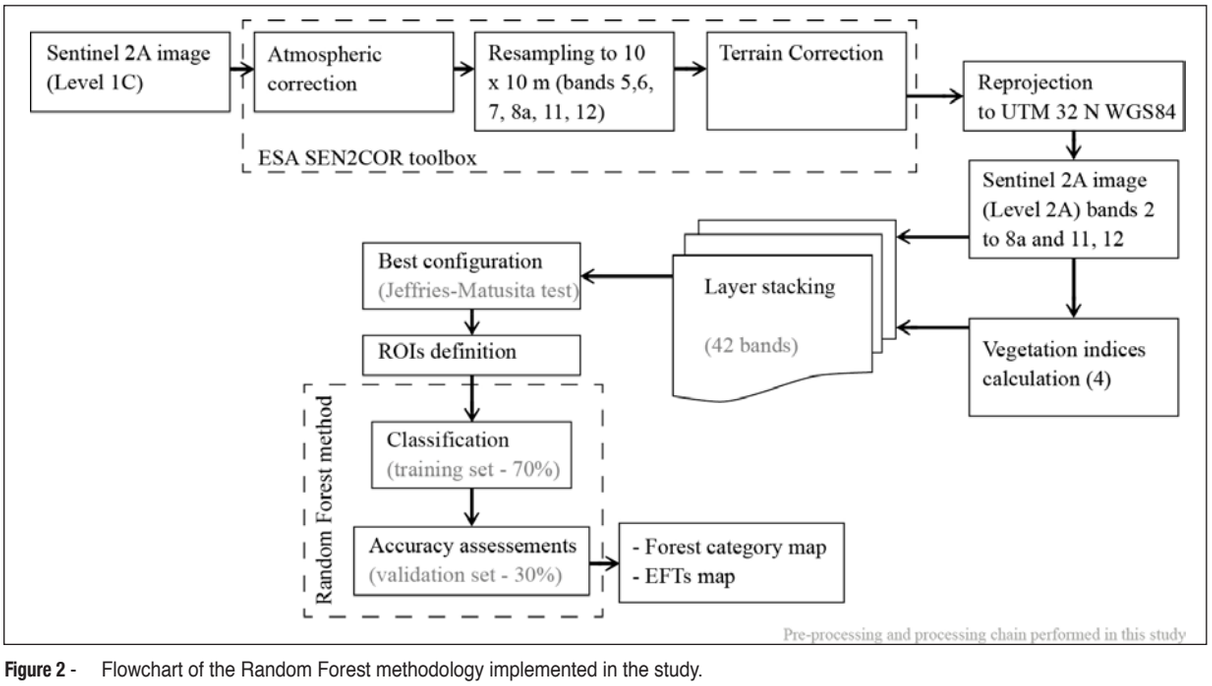

Figure 2 - Flowchart of the Random Forest methodology implemented in the study.

Table 7 - Confusion matrix of the best configuration result (see Table 5) for forest group classification, expressed as number of pixels of the validation set.

pred	true Pure broadleaves	Pure coniferous	Mixed
Pure broadleaves	33,825	526	3,205
Pure coniferous	416	17,383	3,814
Mixed	6,475	7,568	45,571

Table 8 - Confusion matrix of the best configuration result (see Table 6) for EFT classification, expressed as number of pixels of the validation set. EFT 3.2: Subalpine and mountainous spruce and mountainous mixed spruce-silver fir forest; EFT 7.3: Apennine-Corsican mountainous beech forest; EFT 8.2: Turkey oak, Hungarian oak and Sessile oak forest; EFT 8.7: Chestnut forest.

pred	true EFT 3.2	EFT 7.3	EFT 8.2	EFT 8.7
EFT 3.2	10,919	943	33	476
EFT 7.3	949	34,944	95	776
EFT 8.2	15	26	2,498	120
EFT 8.7	689	880	350	20,029

Table 9 - Accuracy by the Random Forest classifier applied to the validation set of forest groups. CE: Commission Error; OE: Omission Error; PA: Producer Accuracy; UA: User Accuracy.

EFT	CE (%)	OE (%)	PA (%)	UA (%)
Broadleaves	8.43	12.78	91.47	87.22
Coniferous	15.10	22.26	84.90	77.74
Mixed	16.94	10.49	83.06	89.51

Table 10 - Accuracy by the Random Forest classifier applied to the validation set of EFT. CE: Commission Error; OE: Omission Error; PA: Producer Accuracy; UA: User Accuracy. EFT 3.2: Subalpine and mountainous spruce and mountainous mixed spruce-silver fir forest; EFT 7.3: Apennine-Corsican mountainous beech forest; EFT 8.2: Turkey oak, Hungarian oak and Sessile oak forest; EFT 8.7: Chestnut forest.

EFT	CE (%)	OE (%)	PA (%)	UA (%)
EFT 3.2	11.74	13.15	88.26	86.85
EFT 7.3	4.95	5.03	95.05	94.97
EFT 8.2	6.05	16.06	93.95	83.94
EFT 8.7	8.74	6.41	91.26	93.59

step of analysis, only spring and summer images and relative RENDVI have been used to get best results based on J-M scores. Results indicated that the single image bands discriminated well between all considered EFT with exception for forests dominated by oaks and chestnut (Table 6). The inclusion of RENDVI improves the separability between these EFTs.

The best configuration, respectively made of 33 layers (10 bands for winter, 10 for spring, 10 for summer, and the 3 RENDVI) and 22 layers (10 for spring, 10 for summer, and the 2 RENDVI) for forest categories and EFTs, have been separately used as input variables in Random Forest.

3.2. Random forest classification

The confusion matrix and accuracy results are reported in Table 7 and in Table 8. For forest categories, an overall accuracy of 86.2% and a Kappa coefficient of 86.1% have been obtained (Table 9).

For EFTs, an overall accuracy of 92.7% and a Kappa coefficient of 92.6% have been obtained. All the classes reveal comparable producer accuracy, although slightly lower user accuracy was observed in Subalpine and mountainous spruce and mountainous mixed spruce-silver fir forest (Table 10). However, both the PA and UA are above 83% in all the classes. A ranking of variables indicated that the summer bands in Blue, Red-Edge wavelength are the most important for classification (Figure 3).

The validated models were applied to the entire study area and both forest categories and EFTs maps have been produced (Figure 4).

4. Discussion and conclusion

In this study, we demonstrated the effective per-

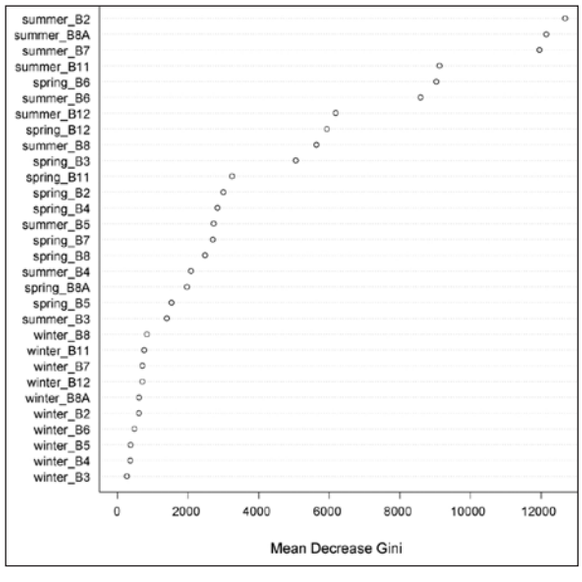

Figure 3 - Random Forest variable importance of S2 bands for EFT classification.

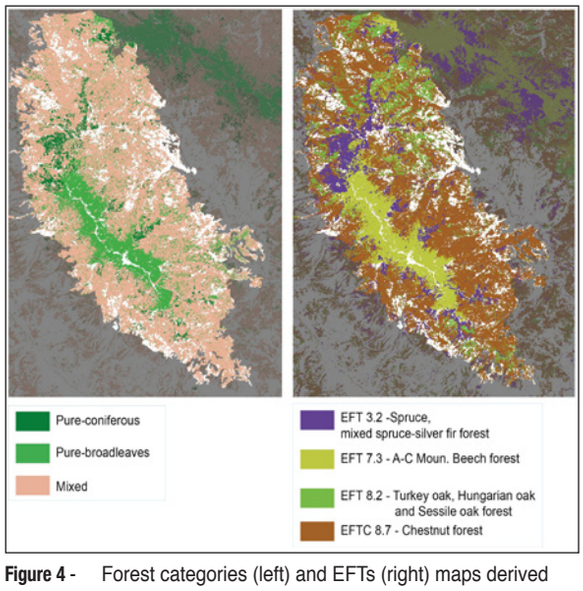

Figure 4 - Forest categories (left) and EFTs (right) maps derived from models prediction over the study area.

formance of S2 in forest mapping based on real operational data under Mediterranean forest environments. We obtained accurate discrimination of EFTs using a single summer image and VIs. We attributed the results mainly to the high spatial resolution available from the 10 m S2 bands and the capability of S2 to include red-edge bands. Indeed, previous studies indicated that using narrow-bands located in the red edge can overcome the well-known problem of saturation of NIR-based vegetation indices (Mutanga et al., 2004). Thus, the availability of four red-edge bands in S2 holds great potential to improve the applicability of optical remote sensing of forests compared with past satellite data (Sellers, 1985; Todd et al., 1998; Gao et al., 2000; Thenkabail et al., 2000).

At another level, we observed that single image data was not able to significantly discriminate forests categories nor forest types, unless VIs are included in the analysis. As expected, the inclusion of multitemporal data gave best results in the classification.

The use of ESA corrected images (L1C level) allows robust S2 product derivation which is prerequisite for standardizing the protocol of image processing and allows comparability among future studies involving operational S2 data.

We conclude that S2 data have been proved to be suitable for routine, medium to large scale mapping and monitoring of forest changes due to the combination of high spatial resolution and quick revisit time.

Acknowledgments

The study was supported by the Project "AL-ForLab" (PON03PE_00024_1) co-funded by the Italian Operational Programme for Research and Competitiveness (PON R,C) 2007-2013, through the European Regional Development Fund (ERDF) and national resource (Revolving Fund - Cohesion Action Plan (CAP) MIUR).

References

Adelabu, S., Mutanga, O., Adam, E., Cho, M.A., 2013. *Exploiting machine learning algo- rithms for tree species classification in a semiarid woodland using RapidEye image.* J. Appl. Remote. Sens. 7 (1) (073480–1–073480–13).

Baillarin S.J., Meygret A., Dechoz C., Petrucci B., Lacherade S., Tremas T., Isola C., Martimort P. Spoto F. 2012 - *Sentinel-2 level 1 products and image processing performances.* IEEE International Geoscience and Remote Sensing Symposium, 7003-7006.

Bajocco S., Raparelli E., Patriarca F., Di Matteo G., Nardi P., Perini L., Salvati L., Mugnozza G.S.,2013 - *Exploring forest infrastructures equipment through multivariate analysis: complementarities, gaps and overlaps in the Mediterranean basin.* Annals of Silvicultural Research 37(1):1-6. doi: 10.12899/asr-774.

Barbati A., Marchetti M., Chirici G., Corona P. 2014 - *European forest types and forest Europe SFM indicators: tools for monitoring progress on forest biodiversity conservation.* Forest Ecology and Management 321: 145-157.

Bartholomé E., Belward A.S. 2005 - *GLC2000: A new approach to global land cover mapping from Earth observation data.* International Journal of Remote Sensing 26: 1959–1977.

Breiman L. 2001 - *Random forests.* Machine Learning, 45(1): 5–32.

Chianucci F. 2016 – *A note on estimation canopy cover from digital cover and hemispherical photography.* Silva Fennica 50, doi: 10.14214/sf.1518

Chianucci F., Cutini A. 2013 - *Estimation of canopy properties in deciduous forests with digital hemispherical and cover photography.* Agricultural and Forest Meteorology 168: 130-139.

Chianucci F., Disperati L., Guzzi D., Bianchini D., Nardino V., Lastri C., Rindinella A., Corona P. 2016 - *Estimation of canopy attributes in beech forests using true colour digital images from a small fixed-wing UAV.* International Journal of Applied Earth Observation and Geoinformation 47: 60-68.

Chianucci, F., Puletti, N., Venturi, E., Cutini, A. and Chiavetta, U. 2014. *Photographic assessment of overstory and understory leaf area index in beech forests under different management regimes in Central Italy.* Forestry Studies, 61(1), pp.27-34.

Cinnirella S., Magnani F., Saracino A., Borghetti M. 2002 - *Response of a mature Pinus laricio plantation to a three-year restriction of water supply: structural and functional acclimation to drought.* Tree Physiology 22(1): 21-30.

Congalton R. G. 1991 - *A review of assessing the accuracy of classifications of remotely sensed data.* Remote Sensing of Environment 37: 35–46.

Davi H., Soudani K., Deckx T., Dufrene E., Le Dantec V., Francois, C. 2006 - *Estimation of forest leaf area index from SPOT imagery using NDVI distribution over forest stands.* International Journal of Remote Sensing 27: 885–902.

Fassnacht F.E., Latifi, H., Stereńczak K., Modzelewska A., Lefsky M., Waser L.T., Straub C., Ghosh A. 2016 - *Review of studies on tree species classification from remotely sensed data.* Remote Sensing of Environment 186: 64-87.

Feddema J.J., Oleson K.W., Bonan G.B., Mearns L.O., Buja L.E., Meehl G.A., Washington W.M. 2005 - *The importance of land-cover change in simulating future climates.* Science 310: 1674–1678.

Foody G. M., Boyd D. S., Cutler M. E. 2003 - *Predictive relations of tropical forest biomass from Landsat TM data and their transferability between regions.* Remote sensing of environment 85(4): 463-474.

Gao X, Huete A.R., Ni W., Miura, T. 2000 - *Optical-biophysical relationships of vegetation spectra without background contamination.* Remote Sensing of Environment 74: 609–620,

Hansen M.C., DeFries R.S., Townshend J.R., Sohlberg R. 2000 - *Global land cover classification at 1 km spatial resolution using a classification tree approach.* International Journal of Remote Sensing, 21(6-7): 1331-1364.

Hill M.J. 2013 - *Vegetation index suites as indicators of vegetation state in grassland and savanna: An analysis with simulated SENTINEL 2 data for a North American transect.* Remote Sensing of Environment 137: 94-111.

Hirose K., Osaki, M., Takeda, T., Kashimura O., Ohki, T., Segah H., Gao Y., Evri, M. 2016 - *Contribution of Hyperspectral Applications to Tropical Peatland Ecosystem Monitoring.* Tropical Peatland Ecosystems (pp. 421-431). Springer Japan.

Immitzer, M., Atzberger, C., Koukal, T., 2012. *Tree species classification with random Forest using very high spatial resolution 8-Band WorldView-2 satellite data.* Remote

Sens. 4 (9), 2661–2693.

Immitzer M., Vuolo F., Atzberger C. 2016 - F*irst experience with sentinel-2 data for crop and tree species classifications in Central Europe.* Remote Sensing 8(3): 166.

Laurin G.V., Liesenberg V., Chen, Q., Guerriero, L. Del Frate, F., Bartolini, A., Coomes D., Wilebore, B., Lindsell, J., Valentini, R. 2013 - *Optical and SAR sensor synergies for forest and land cover mapping in a tropical site in West Africa.* International Journal of Applied Earth Observation and Geoinformation 21: 7-16.

Laurin G.V., Puletti N., Hawthorne W, Liesenberg V., Corona P. Papale D., Chen Q., Valentini R. 2016 - *Discrimination of tropical forest types, dominant species, and mapping of functional guilds by hyperspectral and simulated multispectral Sentinel-2 data.* Remote Sensing of Environment 176: 163-176.

Liaw A., Wiener M. 2002 - *Classification and regression by randomForest.* R news 2, no. 3:18-22.

Loveland, T.R., Merchant J.W., Brown J.F., Ohlen D.O., Reed B.C., Olson P., Hutchinson J. 1995 - *Map supplement: Seasonal land-cover regions of the United States.* Annals of the American Association of Geographers 85: 339–355.

Maselli F., Moriondo M., Chiesi M., Chirici G., Puletti N., Barbati A., Corona P. 2009 - *Evaluating the effects of environmental changes on the Gross Primary Production of Italian forests.* Remote Sensing, 1(4): 1108-1124.

Moore, M.M., Bauer, M.E., 1990. *Classification of forest vegetation in North-Central Min- nesota using Landsat multispectral scanner and thematic mapper data.* For. Sci. 36 (2), 330–342.

Mutanga O., Skidmore A.K. 2004 - *Narrow band vegetation indices overcome the saturation problem in biomass estimation.* International Journal of Remote Sensing 25: 3999-4014.

Nogueira E.M., Yanai A.M., Fonseca F.O., Fearnside P.M. 2015 - *Carbon stock loss from deforestation through 2013 in Brazilian Amazonia.* Global change biology 21: 1271-1292.

Omruuzun F., Baskurt D.O., Daglayan H., Cetin Y.Y. 2015 - *Utilizing hyperspectral remote sensing imagery for afforestation planning of partially covered areas.* In SPIE Remote Sensing (pp. 96432N-96432N). International Society for Optics and Photonics.

Petropoulos G.P., Kalaitzidis C., Vadrevu K.P. 2012 - *Support vector machines and object-based classification for obtaining land-use/cover cartography from Hyperion hyperspectral imagery.* Computers, Geosciences, 41: 99-107.

Pignatti S., Cavalli R.M., Cuomo V., Fusilli L., Pascucci S., Poscolieri M., Santini F. 2009 - *Evaluating Hyperion capability for land cover mapping in a fragmented ecosystem: Pollino National Park, Italy.* Remote Sensing of Environment 113(3): 622-634.

Puletti N., Camarretta N., Corona P. 2016 - *Evaluating EO1-Hyperion capability for mapping conifer and broadleaved forests.* European Journal of Remote Sensing 49: 157-169.

R Core Team 2017 - *R: A language and environment for statistical computing.* R Foundation for Statistical Computing, Vienna, Austria. URL https://www.R-project.org/.

Richards J.A., Jia X. 1999 - *Remote sensing digital imaging analysis: an introduction.* (3rd ed.). Berlin, Springer.

Sellers P.J. 1985 - *Canopy reflectance, photosynthesis and transpiration.* International Journal of Remote Sensing 6: 1335–1372.

Sellers P.J., Dickinson R.E., Randall D.A., Betts A.K., Hall F.G., Berry J.A., Collatz G.J., Denning A.S., Mooney H.A., Nobre C.A., Sato N. 1997 - *Modeling the exchanges of energy, water, and carbon between continents and the atmosphere.* Science 275: 502–509.

Sophie B., Pierre D. 2009 - *GlobCover 2009 Products Description and Validation Report* European Space Agency: Paris, France, 201

Thenkabail P.S, Smith R.B., De Pauw E. 2000 - *Hyperspectral vegetation indices and their relationships with agricultural crop characteristics.* Remote Sensing of Environment 71: 158–182.

Thimonier A., Sedivy I., Schleppi P. 2010 - *Estimating leaf area index in different types of mature forest stands in Switzerland: a comparison of methods.* European Journal of Forest Research 129: 543-562.

Todd S.W, Hoffer R.M., Milchunas D.G. 1998 - *Biomass estimation on grazed and ungrazed rangelands using spectral indices.* International Journal of Remote sensing, 19: 427–438.

Trumbore S., Brando P., Hartmann H. 2015 - *Forest health and global change.* Science 349: 814-818.

Turner P.D., Cohen W.B., Kennedy R.E., Fassnacht K.S., Riggs J.M. 1999 - *Relationships between leaf area index and Landsat TM spectral vegetation indices across three temperate zone sites.* Remote Sensing of Environment 70: 52–68.

Vaiopoulos A.D., Karantzalos K. 2016 - *Pansharpening on the Narrow Vnir and SWIR Spectral Bands of SENTINEL-2.* ISPRS-International Archives of the Photogrammetry, Remote Sensing and Spatial Information Sciences. 723-730.

Vizzarri M., Chiavetta U., Chirici G., Garfì V., Bastrup-Birk A., Marchetti M. 2014 - *Comparing multisource harmonized forest types mapping: A case study from central Italy.* iForest 8: 59-66. doi: 10.3832/ifor1133-007

Waser, L.T., Küchler, M., Jütte, K., Stampfer, T., 2014. *Evaluating the potential of World- View-2 data to classify tree species and different levels of ash mortality.* Remote Sens. 6 (5), 4515–4545.